Multiquantum vortices in superconductors:
Electronic and scanning tunneling microscopy spectra

S. M. M. Virtanen and M. M. Salomaa

Materials Physics Laboratory, Helsinki University of Technology, P. O. Box 2200 (Technical Physics), FIN-02015 HUT, Finland
(Received 27 August 1999)

Superconducting quasiparticle excitation spectra are computed for m times quantized flux lines using a self-consistent Bogoliubov–de Gennes approach. We find m discrete branches of bound-state solutions in the spectrum, corresponding to different values of the quasiparticle angular momentum. Owing to the bound states, the scanning tunneling microscopy spectrum of the vortex is predicted to display m rows of peaks as a function of the distance from the vortex axis. [S0163-1829(99)04345-3]

Multiply quantized vortices (MQV) have been observed using electron holography in type-I superconducting thin films at high magnetic fields,[1] confirming earlier theoretical predictions.[2] MQV's can also be formed in high-temperature superconductors having columnar or large pointlike defects as pinning centers,[3] and such structures have been argued to be stable in conventional type-II superconductors with attractive columnar defects.[4] Multiquantum vortices, imaged with optical interferometry,[5] are also found in thin films of rotating superfluid ^{4}He. In rotating bulk superfluid ^{3}He, continuous doubly quantized vortices were first detected in the A phase using NMR.[6,7] Moreover, singular doubly quantized vortices with superfluid A_1-phase cores have been predicted to occur in the B phase at high angular velocities.[8]

Quantum-mechanical tunneling has provided crucial experiments on bulk superconductivity. Lately, scanning tunneling microscopy (STM) has enabled the first nanoscale measurements of superconductivity. This probe of mesoscale structures, or scanning tunneling spectroscopy, has revealed fine details within vortex cores.[9] The Bogoliubov–de Gennes (BdG) approach[10] restricted to bound electronic excitations has been applied to account for these features.[11] Especially, the self-consistent method[12] facilitated the interpretation of STM data on singly quantized flux lines and gave an impetus to the renaissance of the wave-function description of inhomogeneous superconductivity.[13]

In this paper the self-consistent BdG method is generalized to multiquantum vortices in s-wave superconductors. We solve the ensuing equations with a fast numerical scheme, allowing us to compute these structures for physically important ranges of parameters inaccessible to previous authors. We determine the spatial variation of the self-consistent superconducting pair potential, the magnetic vector potential, the supercurrent and the full electronic spectrum. In particular, an STM signature characteristic for multiquantum vortices is predicted.

We consider an isolated vortex line with m flux quanta, oriented along the z axis of a cylindrical coordinate system (r,θ,z). We assume isotropic s-wave pairing, and a Fermi surface rotationally invariant about the vortex axis. Hence the system possesses a cylindrical symmetry which, in the gauge where the pair potential $\Delta(\mathbf{r})=|\Delta(r)|e^{-im\theta}$, allows the quasiparticle coherence amplitude to be expressed as

$$\psi_j(\mathbf{r})=\begin{pmatrix} u_j(\mathbf{r}) \\ v_j(\mathbf{r}) \end{pmatrix}=e^{ik_z z}e^{i(\mu-\sigma_z m/2)\theta}\widetilde{f}_j(r). \qquad (1)$$

Here σ_z is the Pauli matrix and $\widetilde{f}_j(r)$ a two-component spinor, the index j labeling different quantum states. The quasiparticle angular momentum quantum number μ is an integer for even m and half an odd integer for odd m.[10] Ansatz (1) yields radial BdG equations

$$\sigma_z \frac{\hbar^2}{2m_\rho}\left\{ -\frac{d^2}{dr^2}-\frac{1}{r}\frac{d}{dr}+\frac{1}{r^2}\left[\mu-\sigma_z\left(\frac{m}{2}+\frac{erA_\theta(r)}{\hbar c}\right)\right]^2 \right.$$
$$\left. -k_F^2+\frac{m_\rho}{m_z}k_z^2 \right\}\widetilde{f}_j(r)+\sigma_x\Delta(r)\widetilde{f}_j(r)=E_j\widetilde{f}_j(r), \qquad (2)$$

where $\mathbf{A}(\mathbf{r})=A_\theta(r)\hat{\theta}$ is the magnetic field vector potential and k_F the Fermi wave number. The contribution of the one-particle potential is modeled by choosing appropriate effective masses m_ρ and m_z, in the plane perpendicular to the vortex axis and along it, respectively, and subsuming its constant contribution into the Fermi energy. The potentials Δ and $\mathbf{A}$ are determined from the implicit self-consistency conditions

$$\Delta(\mathbf{r})=g\sum_{0\leq E_j\leq E_D} u_j(\mathbf{r})v_j^*(\mathbf{r})[1-2f(E_j)], \qquad (3a)$$

$$\mathbf{j}(\mathbf{r})=\frac{e\hbar}{m}\sum_j \mathrm{Im}\{f(E_j)u_j^*(\mathbf{r})D(\mathbf{r})u_j(\mathbf{r})$$
$$+[1-f(E_j)]v_j(\mathbf{r})D(\mathbf{r})v_j^*(\mathbf{r})\}, \qquad (3b)$$

where g is the effective electron-electron coupling constant, f the Fermi function, $E_D=\hbar\omega_D$ the Debye cutoff, $\mathbf{j}(\mathbf{r})$ the supercurrent density, and $D(\mathbf{r})=\mathbf{\nabla}-(ie/\hbar c)\mathbf{A}(\mathbf{r})$ the gauge covariant derivative.

Following Gygi and Schlüter,[12] we solve Eq. (2) in a cylinder of radius R applying an iterative scheme: At each iteration step, new potential functions are calculated using Eqs. (3a) and (3b), combined with Maxwell's equation $\mathbf{\nabla}\times\mathbf{\nabla}\times\mathbf{A}=(4\pi/c)\mathbf{j}$, until convergence is achieved. The radius R is chosen large enough for finite-size effects to be
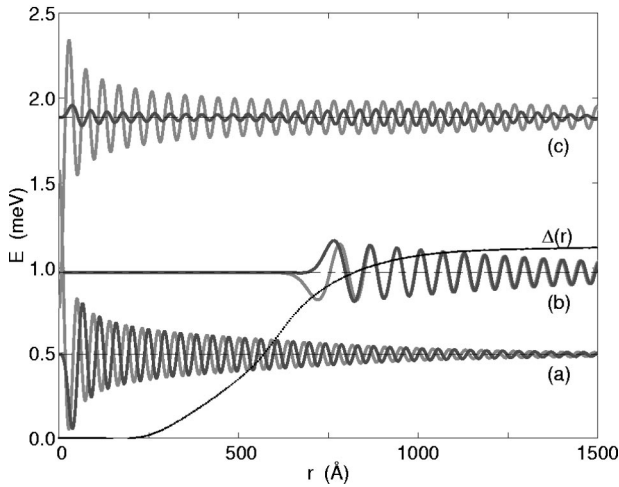
FIG. 1. Self-consistent electronic excitations in an axisymmetric vortex with $m=4$ flux quanta (cf. Ref. 1, Fig. 16). Quasiparticle amplitudes $u(r)$ and $v(r)$ are denoted with blue and red curves, at the respective eigenenergies. The corresponding pair potential $\Delta(r)$ is indicated with the dotted curve (cf. Fig. 2). Bound states with (a) $\mu=2$, (b) $\mu=100$, and a scattering state for (c) $\mu=2$.

negligible, and in particular much larger than the coherence length ξ and the magnetic-field penetration depth λ. We use a finite-difference method to transform Eq. (2) into an eigenvalue problem. Eigensolutions below the Debye cutoff are calculated employing the Lanczos method.[14] The computing time scales with N, the number of discretization lattice points, only approximately linearly. This is to be contrasted with the Bessel function expansion method applied in Refs. 12 and 15, leading to a computing time scaling as $(N_d)^p$ with $p \approx 3$; here N_d is the number of degrees of freedom in the discretization. This difference in scaling implies superiority of our method for large $k_F R$.[16]

The materials parameters in our computations were chosen appropriate for NbSe$_2$. We assumed a cylindrical Fermi surface ($m_z \gg m_\rho$), so that the k_z dependence in Eq. (2) may be neglected. We chose a Debye cutoff $E_D=3.0$ meV, an effective mass $m_\rho=2m_e$, and a Fermi energy E_F
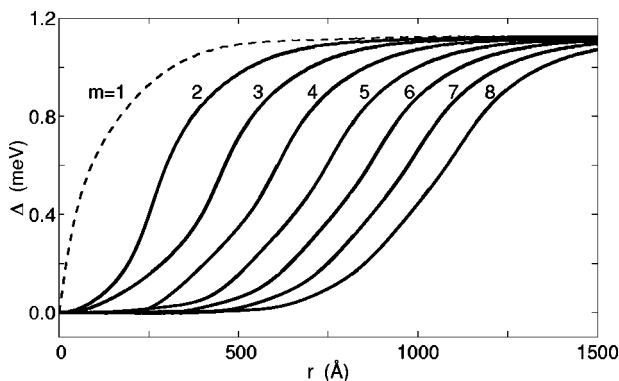

FIG. 2. Iterated self-consistent pair potentials for axisymmetric multiquantum vortex lines with $m=2,\ldots,8$ at $T=1.5$ K. The singly quantized vortex structure (dashed) agrees with the calculations of Ref. 12. In the quantum limit $T \rightarrow 0$, the pair potentials (Refs. 15 and 20) differ qualitatively from the Ginzburg-Landau form; here these features are barely distinguishable.
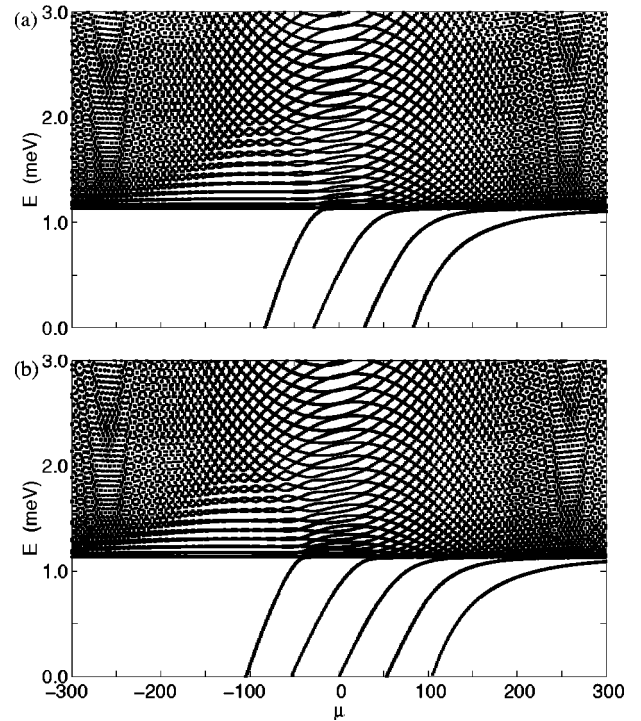

FIG. 3. Parts of the computed discrete self-consistent energy spectra for quasiparticles in vortices with (a) $m=4$ and (b) $m=5$ flux quanta. Note the m discrete branches of bound states below $\Delta_\infty=1.12$ meV.

$=37.3$ meV corresponding to velocity $v_F=8.1\times10^6$ cm/s. The coupling constant g was chosen to correspond to a bulk energy gap of $\Delta_\infty \equiv \Delta(r=R)=1.12$ meV and a critical temperature $T_c \approx 7.4$ K. These values, especially that of the effective mass, are not optimized to the experimental data on singly quantized vortices;[9] however, we argue that qualitatively the results remain invariant within a wide range of parameter values.[17]

The radius of the domain was set to $R=6000$ Å, twice the value used in Ref. 12. The supercurrent density calculated from Eq. (3b) was fitted at a radius r_c, where the self-consistent current density has decreased to 2.5% of its peak value, to a general Ginzburg-Landau form $CK_1(r/\lambda)$; here K_1 is the modified Bessel function, C a constant to be determined, and λ the penetration depth calculated for the singly quantized vortex using a fitting interval of 500 Å.[18]

Results of self-consistent calculations at the temperature $T=1.5$ K are shown in Figs. 1–4. Figure 1 displays the amplitudes $u(r)$, $v(r)$ of three quasiparticle eigenstates in a vortex with $m=4$ flux quanta. States (a) and (b) are exponentially decaying bound states below Δ_∞ while (c) is a scattering state. On the vortex axis, the amplitudes behave asymptotically as $u(r)\sim r^{|\mu-m/2|}$ and $v(r)\sim r^{|\mu+m/2|}$. They display maxima at approximately $r \simeq |\mu|/k_F$, in accordance with the angular momentum of the states. The self-consistent pair-potential amplitudes $\Delta(r)$ for $m=2,\ldots,8$ flux quanta are presented in Fig. 2. Our results are in accordance with the asymptotic Ginzburg-Landau form $\Delta(r)\sim r^m$ ($r \lesssim \xi$); however, quantum effects manifest at low temperatures[20] are discernible already at $T=1.5$ K considered here.
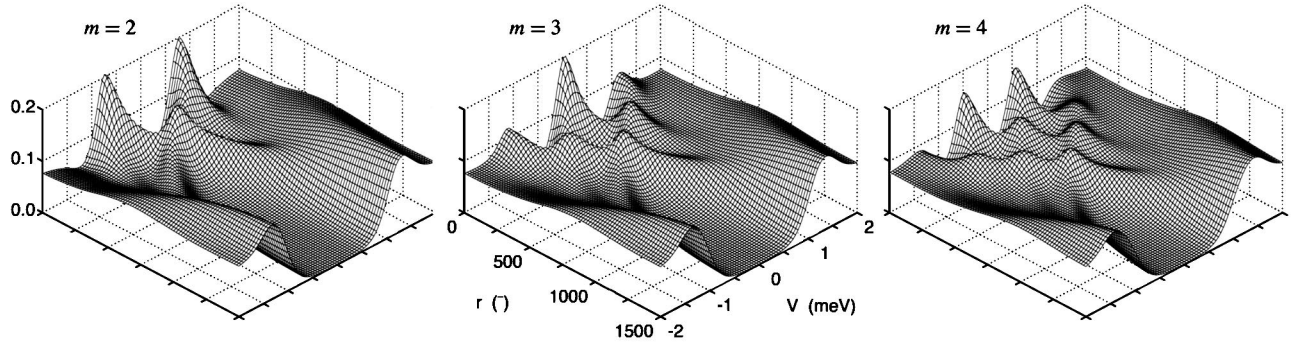
Figure 3 shows parts of the self-consistent energy spectra

FIG. 4. Computed tunneling conductances for vortex lines with $m=2$, 3, and 4 flux quanta exhibit m rows of peaks as functions of the radial distance r from the vortex axis, in triangular patterns. This predicted structure and number of the tunneling maxima in the STM conductance spectrum would serve as a fingerprint for the number of flux quanta enclosed by a vortex line.

calculated for flux lines with $m=4$ and 5 flux quanta. They exhibit an interesting feature which we argue to hold generally: the quasiparticle spectrum for a vortex line with m flux quanta has exactly m bound-state branches, for fixed k_z, as a function of μ. We have checked this numerically for $m=1,\ldots,20$ with various parameter values. This characteristic can also be derived analytically: Generalizing the calculation of Bardeen et al.[19] (based on the WKBJ approximation) to multiply quantized vortices, one finds that the values of μ where the bound-state branches cross the $E=0$ axis for $k_z=0$ are given approximately as

$$\mu \simeq k_F r_\Delta \cos\left[\left(\frac{1}{2}+l\right)\frac{\pi}{m}\right]; \quad l=0,1,\ldots,\left\lfloor\frac{m-1}{2}\right\rfloor. \quad (4)$$

Here r_Δ is the half depth radius of the pair potential well at the core, and $\lfloor\ \rfloor$ denotes rounding downwards to the preceding integer. In the detailed derivation,[20] the potential well is assumed to be steep. Formula (4) yields the locations of the branches in agreement with our self-consistent calculations, except for the outermost branches for large m. More importantly, Eq. (4) predicts the total number of the branches to equal m. It is to be noted that this property in no way depends on the exact form of the pair potential, as long as r_Δ is not too small.

The m bound-state branches of the quasiparticle spectrum lead to a peculiar multipeak structure in the tunneling conductance, that we suggest to be measured with STM experiments. The computed differential conductance[12]

$$\frac{\partial I}{\partial V} \propto -\sum_j \{|u_j(\mathbf{r})|^2 f'(E_j-eV) + |v_j(\mathbf{r})|^2 f'(E_j+eV)\},$$
$$(5)$$

where V is the bias voltage, is presented in Fig. 4 for the multiquantum flux lines with $m=2$, 3, and 4 (see Ref. 12 for $m=1$). The conductance maxima arise from the structure of the bound-state branches in the corresponding energy spectra: as noted above, the quasiparticle probability amplitudes $|u(\mathbf{r})|^2$ and $|v(\mathbf{r})|^2$ have maxima at $r \simeq |\mu|/k_F$, while the derivative of the Fermi function is peaked at zero energy. Hence, for given (r,V), the principal contribution to the tunneling conductance originates from states with $(|\mu|,E)$ $=(k_F r, |eV|)$. In the bound-state region, there usually is only a single state satisfying this condition, but for certain (r,V) there occur two such states, situated symmetrically about $\mu=0$. This results in local maxima in the differential conductance. On the other hand, for states with $E \approx 0$, both the u and v components of the quasiparticle amplitudes contribute to the conductance at the same point, also giving local maxima; this explains the prominent peaks at $(r,V)=(0,0)$ for odd m. Altogether, the m bound-state branches generate a wedge-shaped pattern of maxima in the differential conductance, consisting of m rows of peaks as a function of r.[21] These are clearly displayed in Fig. 4.

In bulk superconductors, multiquantum vortices can be stabilized by columnar defects.[22] We have also studied the effect of such material inhomogeneities on the electronic structure of vortices, finding that the predicted qualitative features of STM spectra are essentially modified only in insulating regions of the defects. Especially, for defects with normal metallic conductivity the multipeak STM signature remains. The results are expected to be relevant also for multiquantum vortices in thin films of type-I materials, for which the homogeneity approximation can be essentially compensated by using effective materials parameters of type-II superconductors. Experimental observations of multiquantum vortices has been difficult due to the requirement of simultaneous high spatial resolution and magnetic-flux sensitivity of the measurements.[1] However, we propose that the magnetic flux of multiquantum vortices can in fact be counted from the predicted tunneling peaks exactly, merely using the excellent spatial resolution of scanning tunneling microscopy.

In conclusion, we have solved the Bogoliubov–de Gennes equations numerically for axisymmetric multiply quantized vortices using a fast computational scheme. The energy spectrum for vortices with m flux quanta exhibits exactly m bound-state branches as a function of the quasiparticle angular momentum; we argue this to be valid generally. The specific structure of the bound-state part of the spectrum leads to a characteristic multipeak structure in the computed differential conductance. We suggest an experimental search for these distinct STM fingerprints of multiquantum vortices.

[1] S. Hasegawa, T. Matsuda, J. Endo, N. Osakabe, M. Igarashi, T. Kobayashi, M. Naito, A. Tonomura, and R. Aoki, Phys. Rev. B **43**, 7631 (1991).

[2] G. Lasher, Phys. Rev. **154**, 345 (1967).

[3] A. I. Buzdin, Phys. Rev. B **47**, 11 416 (1993); I. B. Khalfin and B. Ya. Shapiro, Physica C **202**, 393 (1992); M. Baert, V. V. Metlushko, R. Jonckheere, V. V. Moshchalkov, and Y. Bruynseraede, Phys. Rev. Lett. **74**, 3269 (1995).

[4] G. M. Braverman, S. A. Gredeskul, and Y. Avishai, Phys. Rev. B **57**, 13 899 (1998).

[5] P. L. Marston and W. M. Fairbank, Phys. Rev. Lett. **39**, 1208 (1977).

[6] O. T. Ikkala, G. E. Volovik, P. J. Hakonen, Yu. M. Bun'kov, S. T. Islander, and G. A. Kharadze, Pis'ma Zh. Éksp. Teor. Fiz. **35**, 338 (1982) [JETP Lett. **35**, 416 (1982)].

[7] For a comprehensive review, see D. Vollhardt and P. Wölfle, *The Superfluid Phases of Helium 3* (Taylor & Francis, London, 1990).

[8] M. M. Salomaa and G. E. Volovik, Phys. Rev. Lett. **52**, 2008 (1984).

[9] H. Hess, R. B. Robinson, R. C. Dynes, J. M. Valles, Jr., and J. Waszczak, Phys. Rev. Lett. **62**, 214 (1989); H. F. Hess, in *Scanning Tunneling Microscopy*, edited by J. A. Stroscio and W. J. Kaiser (Academic Press, New York, 1993), p. 427.

[10] P. G. de Gennes, *Superconductivity of Metals and Alloys* (Addison-Wesley, Reading, MA, 1989).

[11] J. D. Shore, M. Huang, A. T. Dorsey, and J. P. Sethna, Phys. Rev. Lett. **62**, 3089 (1989).

[12] F. Gygi and M. Schlüter, Phys. Rev. B **41**, 822 (1990); **43**, 7609 (1991).

[13] I. Kosztin, Š. Kos, M. Stone, and A. J. Leggett, Phys. Rev. B **58**, 9365 (1998).

[14] We used software available from the ARPACK Home Page at Comp. and Appl. Math. Dept., Rice Univ., http://www.caam.rice.edu/software/ARPACK

[15] N. Hayashi, T. Isoshima, M. Ichioka, and K. Machida, Phys. Rev. Lett. **80**, 2921 (1998).

[16] To obtain a preassigned numerical accuracy, note that both N and N_d scale linearly with $k_F R$. Due to the increase in the density of scattering states with the radius R of the computational region, the execution time varies as $\sim R^2$ for fixed E_D; nevertheless, this is quite advantageous in comparison to the Bessel function expansion method.

[17] We have also made computations with much larger k_F and m_ρ, varying the coupling constant g, and found qualitative agreement with the results presented here.

[18] The asymptotic behavior of the current density yielded $\lambda = 640$ Å for temperatures $T \ll T_c$. The fitting point r_c is a measure for the size of the vortex, ranging from 1680 Å ($m=1$) to 3550 Å ($m=8$) at low temperatures. Correspondingly, the maximum absolute values of the quantum number μ for which Eq. (2) has to be solved to ensure full convergence in this region vary in the range 250–500.

[19] J. Bardeen, R. Kümmel, A. E. Jacobs, and L. Tewordt, Phys. Rev. **187**, 556 (1969).

[20] S. M. M. Virtanen and M. M. Salomaa (unpublished).

[21] For vortices with $m=2$, 3, or 4 flux quanta, there also occur exactly m peaks in the STM spectrum on the vortex axis as a function of the tunneling voltage. However, for larger m the outermost branches merge into the scattering continuum of the spectrum before crossing the $\mu=0$ line, and the corresponding conductance maxima disappear. See also D. Rainer, J. A. Sauls, and D. Waxman, Phys. Rev. B **54**, 10 094 (1996), where the local density of states for a doubly quantized vortex line has been presented at $r=0$ within quasiclassical theory.

[22] By computing the microscopic free energy of the vortices, we have demonstrated (Ref. 20) that multiquantum flux lines can be stabilized by columnar defects in conventional type II materials also near H_{c_1} (cf. Ref. 4).